Location of cavities buried in the Neapolitan Yellow Tuff using the seismic reflection method

P. P. BRUNO and A. RAPOLLA

Dipartimento di Geofisica e Vulcanologia, Università Federico II, Napoli, Italy

(Received January 9, 1995; accepted September 28, 1995)

Abstract. A shallow seismic reflection survey was carried out at two sites near the city of Naples, where a large number of cavities have been dug over the past centuries into the Yellow Tuff Formation. To predict the response of the ground-cavity system to the seismic pulse, 2D synthetic wave propagation seismograms were produced using forward modelling theory. Then the seismic data were processed in two different ways to search for the diffraction hyperbolae generated by the cavity, and for any breaks in seismic reflectors below the area where the cavity is located. At the first site (Frattaminore), we were able to detect the diffraction hyperbolae, and with them to calculate the depth of the cavity. Here, we could also record the reflection from the top of the volcanic tuff; but, because of the complex environment and of the data quality, deeper reflections were not well visible on the seismogram. Thus, in order to improve the temporal resolution of the records and their signal-to-noise ratio, the data were processed by deconvolution and F-K dip-filtering. After this other, deeper events appeared on the section, but not in the depth range of the cavity. Despite the similar geological conditions of the two sites, it was not possible to record good seismic data at Grumo Nevano, due to the different environmental noise.

1. Introduction - Geological settings

Below Naples and part of its hinterland there is a large number of cavities, excavated in the past in the Yellow Tuff to extract material for building. The location of many of these cavities is unknown, and this is a source of potential risk in both human and financial terms. Therefore, there is a need for methods that give information on the site conditions and that can show continuous data (e.g. profiles) rather than isolated single point data. The seismic reflection method has

Corresponding author: P. P. Bruno; Dipartimento di Geofisica e Vulcanologia, Università Federico II, Largo S. Marcellino 10, 80138 Napoli, Italy; Tel. +39 81 5803113; Fax +39 81 5527 631; e-mail: bruno@dgoma.dgv.umima.it

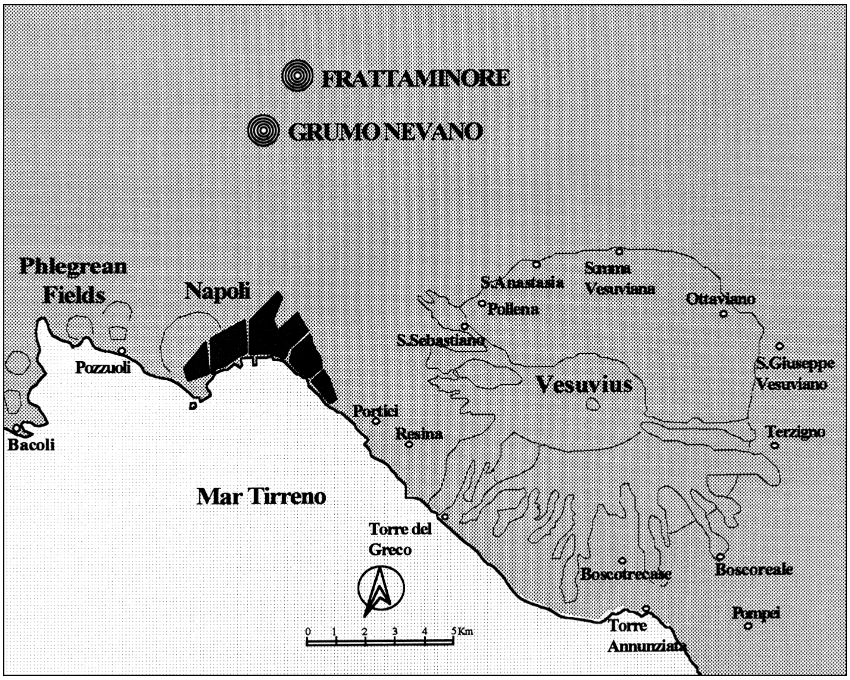

Fig. 1 - Location of the test sites.

been used in the recent times for the detection of cavities, with varying results. The additional difficulty found in our case is essentially due to the following factors.

- *Geological factor.* The majority of the cavities are located in volcanic rocks whose shallow part consists of incoherent and dry pyroclastic material, which has a strong attenuation coefficient for seismic wave propagation.
- *Environmental factor*. Most of the areas where these cavities were dug are nowadays urbanised. This results in a high environmental noise level and, in some cases, even lack of space for surveying.

Two sites, in the towns of Grumo Nevano and Frattaminore, which seemed suitable for testing the method, were chosen. Their locations are shown in Fig. 1. The pyroclastic lithotypes occurring in both areas came from the volcanic activity of the Phlegrean Fields and the Somma-Vesuvius. The *Neapolitan Yellow Tuff* formation, deposited about 12,000 years ago after a large explosive eruption in the Phlegrean Fields, is generally found at both sites beneath 10÷12 m of undifferentiated volcanic products, mainly ash, sand and lapilli deposited by recent activity of the two volcanic areas. The stratigraphic columns of the two sites are shown in Fig. 2. At Grumo, the top of a six-meter-high cavity is encountered about 20 m from the surface, and about 10 m under the top of the tuff. The cavity of Frattaminore is also six metres high and eight metres wide. Its roof is found around 13 metres from the surface, only one meter beneath the top of the tuff formation.

The use of shotguns or microcharges as seismic sources over the cavities and in areas with intense urbanisation had to be avoided. Since at both sites the ground was compact enough, a 5

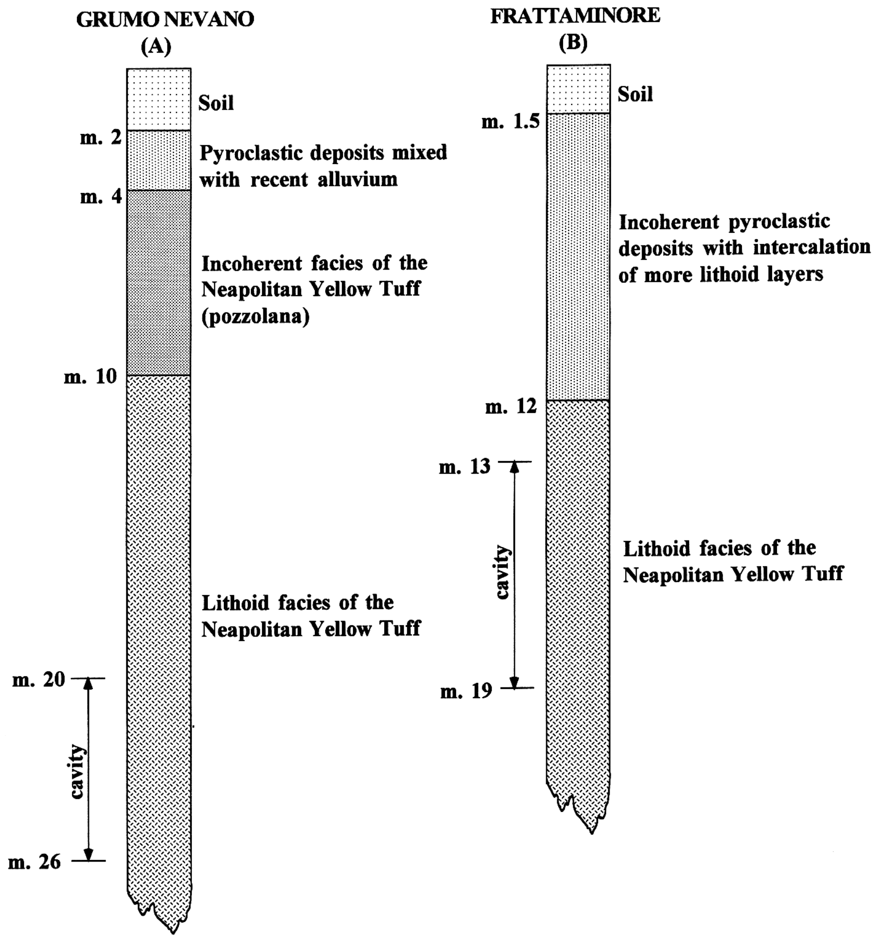

Fig. 2 - Stratigraphic columns for Grumo Nevano (a) and Frattaminore (b).

kg sledgehammer was chosen. The seismograph used was a simple 12-channel EG&G 1225 GEOMETRICS. The data were recorded in digital format on 3 1/2-inch magnetic diskettes. Analog-to-digital (A/D) conversion resulted in a word length of 8 bits plus sign. The trace lengths recorded at Grumo Nevano were 100 ms with a sample interval of 0.1 ms, and 250 ms with a sample interval of 0.25 ms. At Frattaminore, only a record length of 250 ms was chosen. At both places, twelve 100-Hz vertical geophones were deployed to reduce the presence of ground roll on the seismic records.

2. Modelling

To predict the seismic response of a cavity, a simulation test, based on *finite-difference* (FD) theory was run. Finite-difference techniques are particularly attractive for structurally complex subsurface geometries, because boundary conditions at lithological contacts are properly and

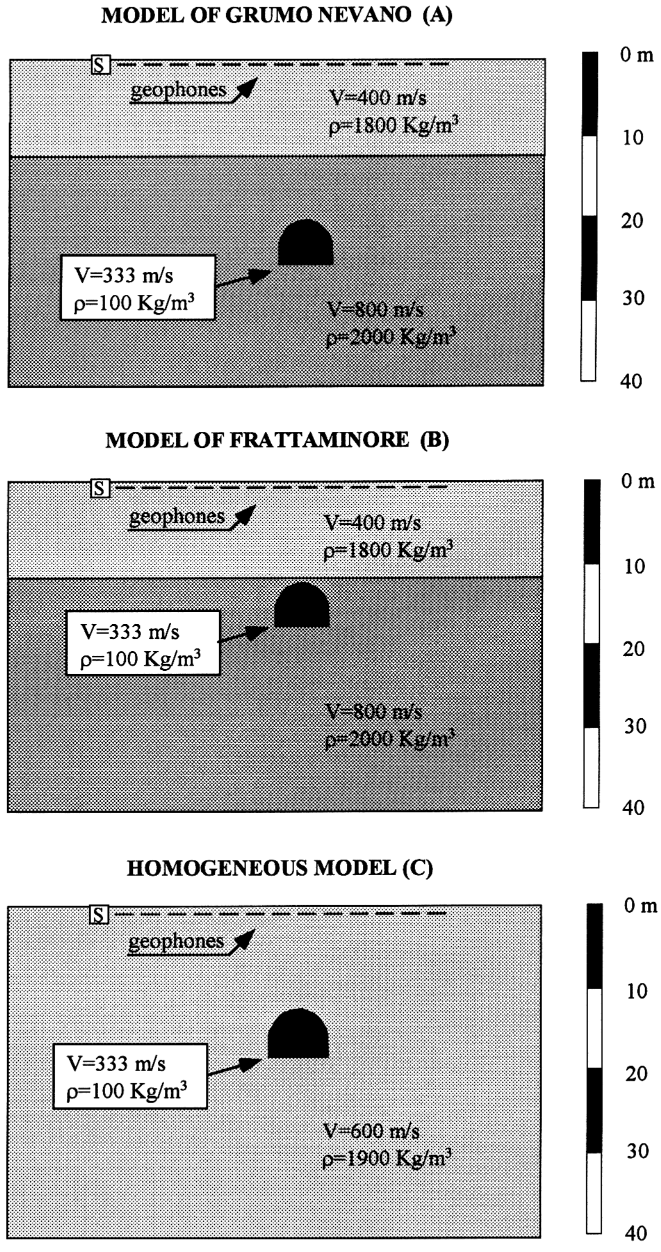

Fig. 3 - Geological two-dimension models utilised for the derivation of the P-wave synthetic seismograms. The location of the point source (for the synthetic walkaway noise experiment) and the mechanical properties of the models are as indicated in the drawing. For the 2D plane-wave experiment, the line source was deployed along the top sides of the models. S=source; V=acoustic wave velocity; ρ=density.

automatically accounted for by the operator. Finite-difference techniques approximate the two-dimensional differential wave equation with difference equations, which are iteratively solved on a discrete spatial grid. We used a FORTRAN program (FINMODEL.FOR), written by

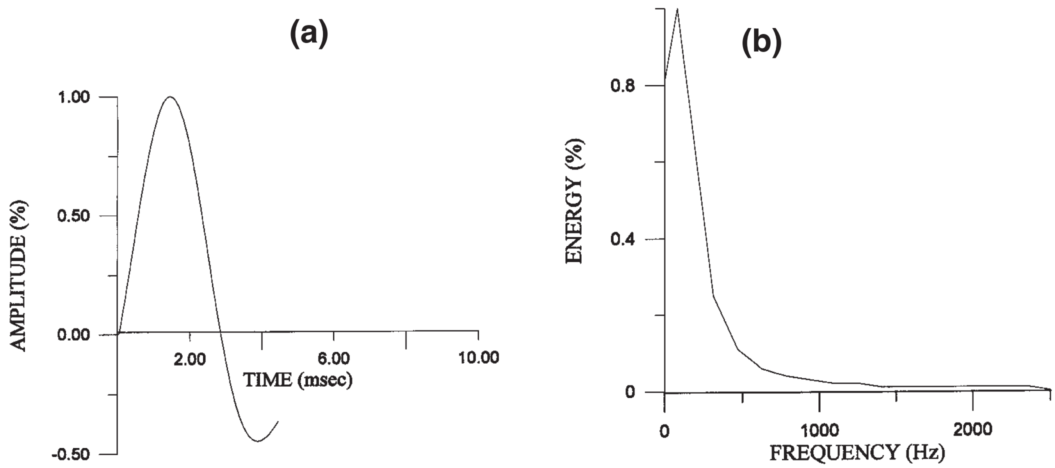

Fig. 4 (a) Synthetic source function. (b) Synthetic source power spectrum.

Keiswetter and Black (1994), for numerical approximation of the 2-D scalar wave equation valid in a heterogeneous medium. Such a medium allows the velocity and density to vary with spatial location, and the formulation of the equation implicitly satisfies the boundary conditions at every point in the model. Although the FD technique has been described by previous researchers, FINMODEL is, to our knowledge, the first complete working program for a PC ever published. This program uses explicit approximations of second-order accuracy for both the spatial and temporal sampling intervals. The geologic model input to the FD equation must be restricted to a finite number of grid points, due to computer memory limitations. Unwanted reflections from the bottom and sides of the model have received considerable attention, and various techniques have been developed to reduce them (Clayton and Engquist, 1977; Reynolds, 1978; Sochacki et al., 1987; Keys, 1985). Keiswetter and Black used artificial boundary conditions, described by Reynolds (1978), that separate the wavefield according to the direction of travel.

To generate a synthetic model, three steps are needed: i) create a geological grid model (Δx, Δz); ii) assign to each cell of the model its velocity and density; iii) define the model parameters and the source-geophone geometry.

The models utilized for the simulation are drawn in Fig. 3. Each model is a grid of 400x250 square cells with side of 0.2 m. Unlike the other three sides, the top is not absorbing, so we get multiple reflections and diffractions in the data. For all the models, the point source is located at node n. 68 (indicated by [S] in the drawings of Fig. 3), and the first of the 96 geophones is 3 cells (6 m) from it. The geophone spacing (ΔG) is also 3 cells. Both the source and the geophones are located 2 cells behind the surface. The source function (a Ricker wavelet with a peak frequency of 80 Hz) and the source power spectra are plotted in figure 4. The source time duration is limited to 6 milliseconds for all the numerical simulations. Note that the density of the cavity was taken as 100 kg/m^3 instead of the true value of 1.29 kg/m^3. This is due to limits to the practical application of the FD approximation. As said before, working with finite differences, we substi-

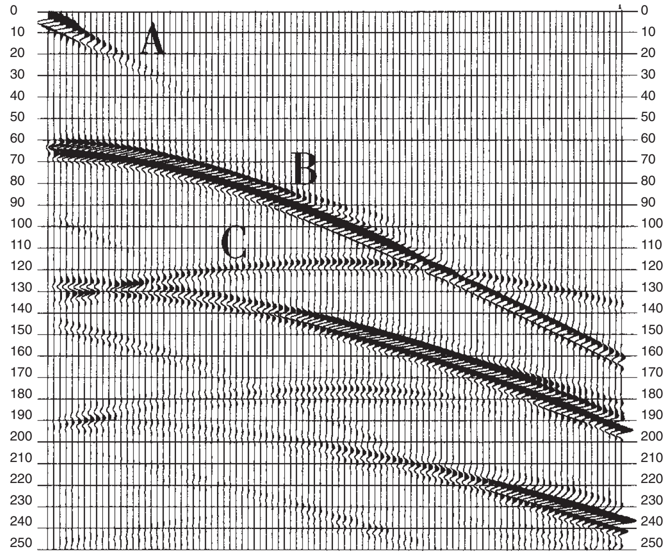

Fig. 5a - Synthetic shot record (time window 0-250 ms - vertical component) for the model of Grumo Nevano. The letters identify: (A) the direct wave; (B) the reflection from the top of the second layer; (C) the diffraction from the cavity. The multiple reflection generated by the wavefront bouncing between the first layer and the ground surface (which is not absorbing), as well as the multiple diffraction reflection generated by the wavefront bouncing between the cavity and the ground surface are clearly visible on this plot and on the others; these events are not labelled. Further energy due to imperfect seismic energy adsorption by the other three sides of the model is visible. Note that the diffracted event is well visible throughout the seismograms.

tute derivatives of the functions by differences calculated between neighbouring nodes. When the gradient is large (i.e., at the passage between the tuff and the cavity), the error created by approximating the two-dimensional differential wave equation by difference equations also becomes large. To overcome this problem, we should reduce the grid spacing (Δx), but there is also a lower limit to Δx. In fact this parameter is also related to the maximum velocity of the medium (C) and the iteration time-step (Δt) in the model stability criteria for heterogeneous media (r) (Kelly et al., 1982) as follows:

$$r = \frac{C\Delta t}{\Delta x} \leq \frac{1}{\sqrt{2}} \cdot \qquad (1)$$

So, if we reduce Δx too much, the model becomes unstable.

The use of a value of 100 kg/m^3, for the density of the cavity, instead of the true value of 1.29 kg/m^3, produces only a negligible difference in the amplitude of the diffracted events. We calculated that for the homogeneous model of Fig. 3c and for vertical incidence, the difference in amplitude is about 5.8%. However, one should still take into account this limit when looking at the modelling results.

The first grid model simplifies the geological features of Grumo Nevano into two seismic layers, having velocity and density as shown in Fig. 3. The second model is similar to the previous with the only difference that the cavity is positioned closer (1 m) to the boundary between

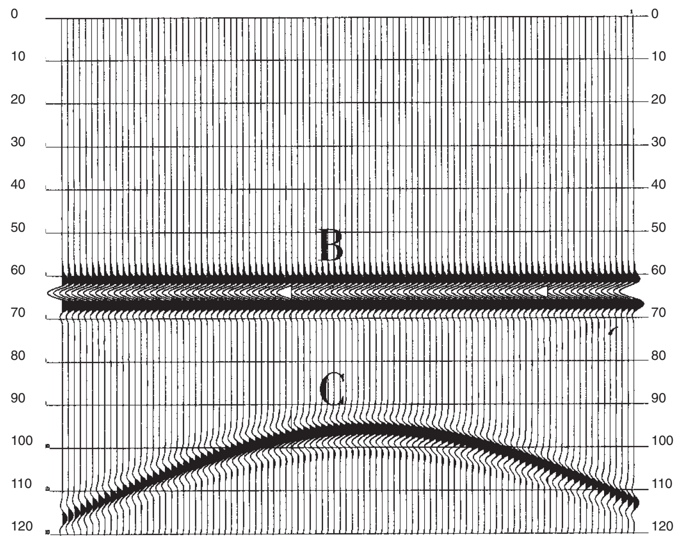

Fig. 5b - Synthetic 2D-plane wave record (time window 0-120 ms - vertical component) for the model of Grumo Nevano. The plane-wave experiments were run in order to simulate how a cavity should show up on a final (stacked) seismic section. The letters label: (B) the reflection from the top of the tuff; (C) the diffraction from the top of the cavity.

the two seismic layers, as in the Frattaminore site. In the third model, the cavity is put in a homogeneous medium having velocities and densities averaged between those of the previous models. This last model was run to understand the effect of the cavity on seismic records without the interference of reflected energy.

The synthetic records (vertical component) are exhibited in Figs. 5-7. We used both a point source, to simulate a field walkaway noise record, and a line source (which generates a 2D plane wave) to simulate a stacked section. Multiple reflections and diffractions coming from the top boundary, and other noise due mainly to the imperfect absorbing condition of the other boundaries, are present on the records. Note in Fig. 7a the event labelled as (D), which is visible only at the geophones located on the extreme right of the model. This event, on the basis of its delay time (around 20 ms), has been interpreted as the wavefront diffracted from the bottom of the cavity. A phase change associated with it is also visible. This is the only synthetic experiment in which the event appeared.

Note that, among the synthetic walkaway records, the worst structural conditions for determination of diffracted energy are represented by that of Frattaminore (Fig. 6a), where the tuff-overburden interface is very close to the roof of the cavity. In this case, most of the diffraction is obscured by the stronger reflected event; in fact, the diffraction hyperbola can only be recognised where it has negative dip; the other part is completely effaced by the reflected event. In a real case, this phenomenon is even more pronounced, because other high-energy events, such as refractions and ground roll, are present on the seismogram. Therefore one can say that detection of a cavity, which is never easy, becomes even more difficult when the cavity is too close to a boundary between different seismic layers. The energy carried by the diffracted waves seems

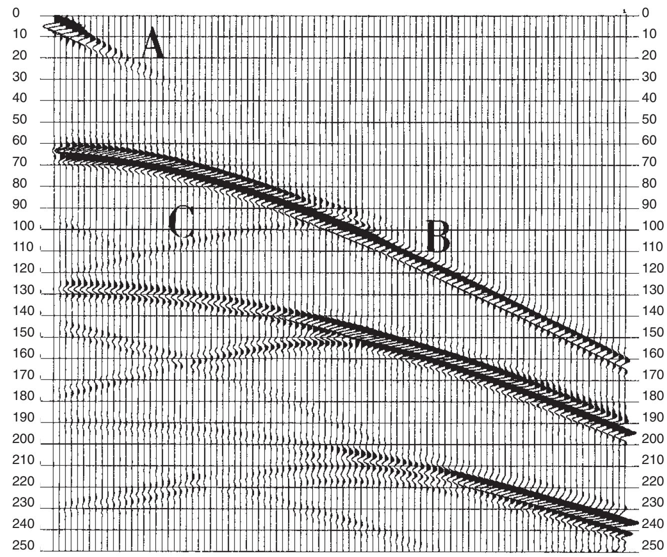

Fig. 6a - Synthetic shot record (time window 0-250 ms - vertical component) for the model of Frattaminore. (A) direct wave; (B) reflection; (C) diffraction. Note that, unlike in the record of Fig 5a, the right side of the diffraction is not visible on the plot. This is due to the closeness of the cavity to the overburden-tuff boundary (only one meter instead of the 10 meters of the corresponding figure for Grumo Nevano). This causes interference between the reflected and the diffracted energy.

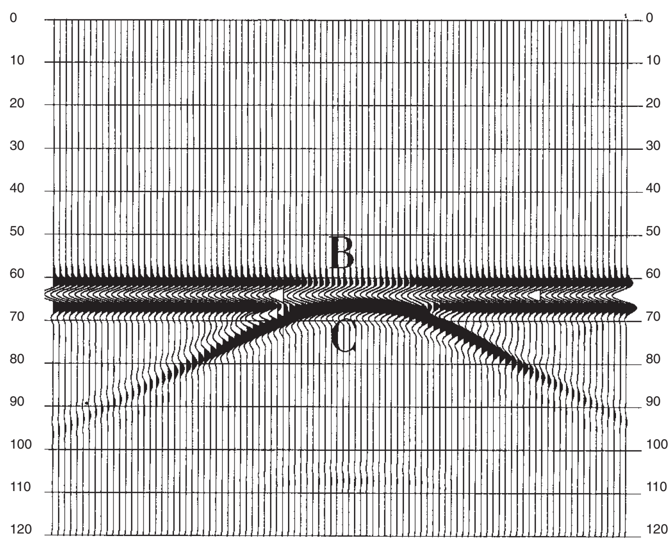

Fig. 6b - Synthetic 2D plane wave record (time window 0-120 ms - vertical component) for the model of Frattaminore. (B) reflection; (C) diffraction. On this synthetic record we can still observe the right side of the diffracted hyperbola. This is due to the greater energy released by the line source in comparison to the point source, and also to the modified ray paths. Nevertheless, the situation of Fig. 6a better focuses the problems encountered in the actual seismic data acquisition at Frattaminore.

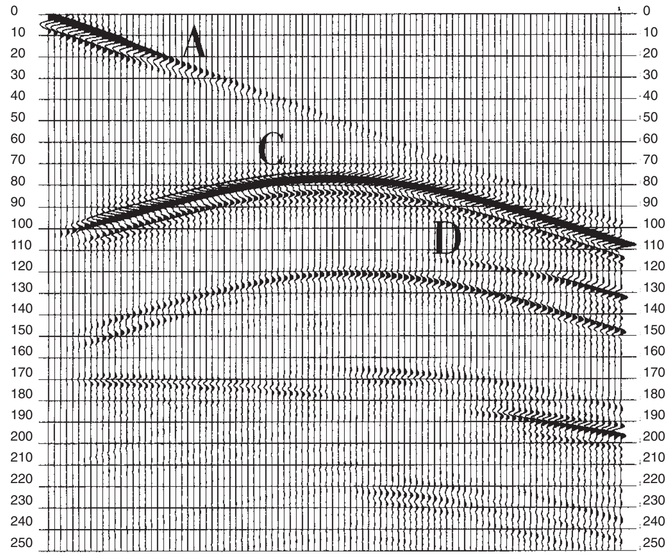

Fig. 7a - Synthetic shot record (time window 0-250 ms - vertical component) for the average model. (A) direct wave; (C) diffraction. The event (D), visible only at geophones located on the extreme right of the model, has been interpreted, on the basis of the delay time (around 20 ms), as the wavefront diffracted from the bottom of the cavity. This is the only synthetic experiment in which the event appeared.

small in comparison to that carried by other kinds of seismic waves, and consequently is difficult to detect in the field, particularly when working with an 8-bit seismograph. In the synthetic plane-wave experiment at Frattaminore (Fig. 6b), the phenomenon is obviously less, because of the use of a line source, but the point-source synthetic record is nearer to the (hard) reality.

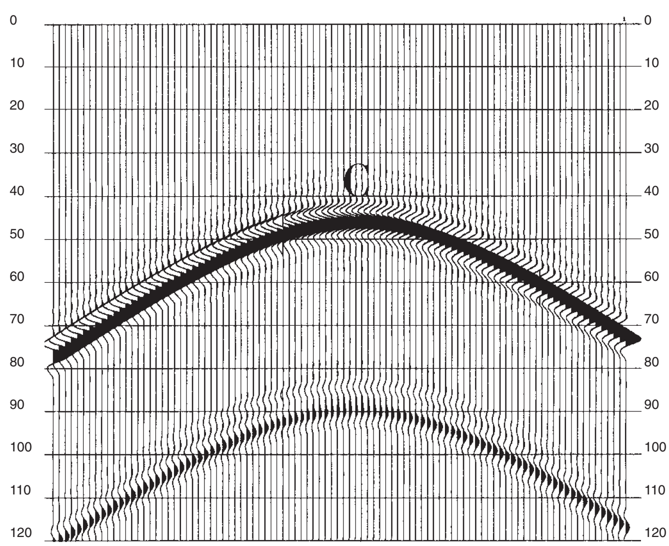

Fig. 7b — Synthetic 2D plane-wave record (time window 0-120 ms - vertical component) for the average model. (C) diffraction.

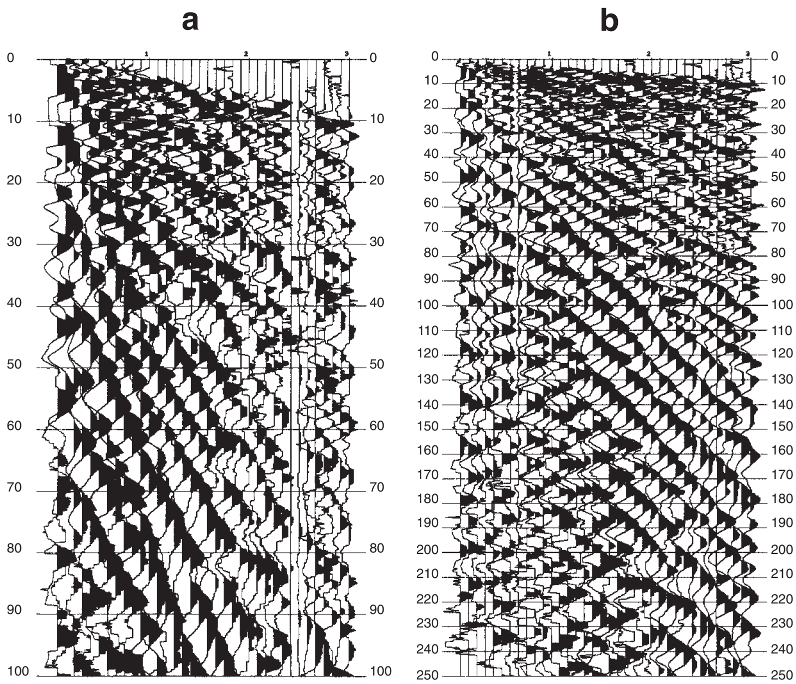

Fig. 8 - Walkaway noise tests for the Grumo Nevano site recorded using a geophone spacing (ΔG) of 0.3 m; (a) record length = 100 ms; (b) record length = 250 ms. Note, at the beginning of the plot, the high frequency wavefront propagating into the 20 cm thick concrete courtyard, and the abundant presence of ground roll throughout the records.

3. Data acquisition and field procedures

Grumo Nevano. The seismic survey included two walkaway noise tests with record lengths of 100 and 250 ms, as shown in Fig. 8, and a single fold 100-ms profile, both along the minor axis of the cavity. The walkaway noise test is critical for the choice of acquisition parameters, such as source offset and geophone spacing, which in this case were set at 3.6 and 0.3 m. On the seismogram the first arrival (having a velocity of about 1200 m/s and frequency around 500 Hz) corresponds to the energy travelling into the 20-cm-thick concrete base of the courtyard. Note also, in the middle of the plots, the abundant ground roll, and seismic noise. The geological setting of the site probably plays a significant role in the generation of these events: the great heterogeneity of the overburden layer covering the tuff basement, together with the presence of building foundations and the concrete basement of the courtyard, creates this high noise level which contaminates the diffractions from the cavity. In this area, therefore, it was impossible to identify and separate the effects of single events.

Frattaminore. The walkaway noise test for in this site is shown is Fig. 9. For this profile a geophone spacing of 0.6 m and a near offset of 26.3 m were chosen. The choice of these field parameters was also influenced by limitations due to site logistics. Some of the records are shown

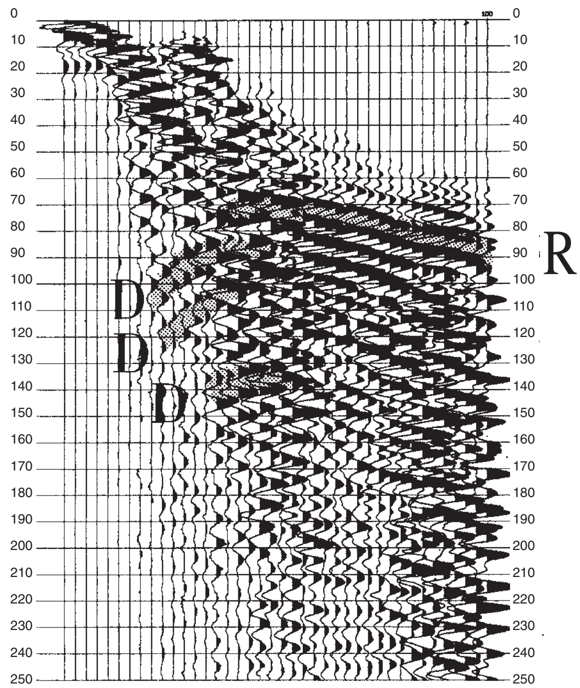

Fig. 9 - Walkaway noise test at Frattaminore recorded using ΔG=0.6 m. (R) reflection from the top of the tuff; (D) diffractions. By comparison of this figure with Fig. 6a, a greater complexity of the actual data, can be noted, of course. In fact we can see at least two hyperbolae on the real data, whose tops are visible around 85 and 115 ms. This last hyperbola could have been generated either by the bottom of the cavity or by other inhomogeneities in the pyroclastic series. If the former is true, the synthetic experiment of Fig. 6a underestimated the resolution obtainable in the field. Note also that the right part of the hyperbolae (having positive dip), as predicted by the synthetic experiment, is not visible on the plot. Other diffractions are perceptible on the records, with more difficulty, at around 135 ms. The origin of these last phenomena can be ascribed to other deeper inhomogeneities in the volcanic series.

in Fig. 10. In both Figs. 9 and 10 we see that the signal is ringing, probably due to the structural complexity of the area. The data processing was aimed at enhancement of the diffraction hyperbolae generated by the cavity, and to individuation of any reflections in the cavity depth range.

4. Data processing and interpretation

Because of the poor quality of the data recorded at Grumo Nevano, the processing reported in this paper regards only the data from Frattaminore. For this site, some of the events are indicated on the walkaway noise test in Fig. 9 (compare this figure with the synthetic 2D shot record of Fig. 6a). The shallower of these events, found between 65 and 85 ms, is the reflection from the top of the tuff basement. The other events marked on the seismogram have been interpreted as diffraction hyperbolae. They cannot be spatial aliasing of ground roll energy because, with the 0.6 m geophone spacing used in the field, the enhanced events, in order to be aliased, would have

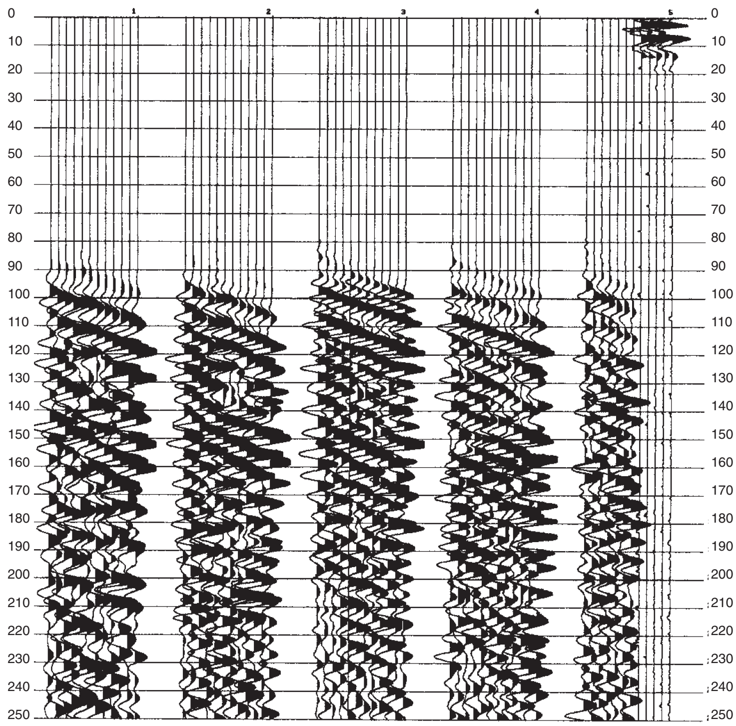

Fig. 10 - Some field records of the profile recorded at Frattaminore with the following parameters: ΔG=0.6 m, ΔS=7.2 m, offset=26.3m. Note that the signal is ringing. The last four traces of the last record are dead, because they were not connected to the geophones in the field, due to the lack of space.

to be much slower. To demonstrate this statement, the shallower of these events was interpolated using the seismic diffraction hyperbola equation (Yilmaz, 1987):

$$t^2(x) = t_0^2 + 4x^2 / V_{RMS}^2; \tag{2}$$

where V_{RMS} is the average (root mean square) of the seismic velocities calculated over the whole ray path. By picking different points for interpolation, a velocity ranging between 390 and 600 m/s was obtained. These velocity values are very different from that of the groundroll.

To calculate the depth to the top of the cavity we read t_o from the seismogram, and used a value of around 400 m/s as V_{RMS} in eq. (2). These values gave us a depth of 16.5 m. As the precise depth of the top of the cavity is uncertain (probably 13±2 m), the value found was satisfactory.

The profile records do not seem to show negative-dip events (whose presence could indicate diffractions). This is easily explained by the fact that we used a near offset of 23.6 m for the field recording, with the geophones positioned over the cavity and the source away from it. With this configuration, it was impossible to record the negative-dip part of the diffraction hyperbolae, as this part arrives only at geophones positioned very close to the source. In fact, looking at the synthetic records of Figs. 5-7, we see that the diffraction hyperbola starts to have a positive dip

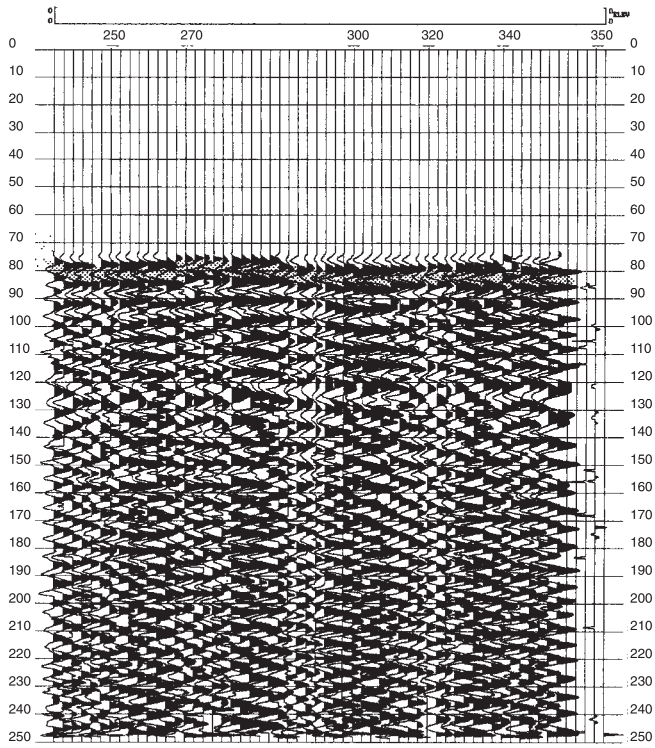

Fig. 11 - Final single-fold section for the site of Frattaminore (with only the 200-Hz high-pass digital filtering and NMO correction applied). The reflection from the top of the tuff is evidenced. The NMO velocities used were: 400 m/s for the first 80 ms, and 800 m/s for the remaining time. Because of the ringing character of the signal no other event, deeper than the reflection described above, is visible on this plot.

at a distance of 18-20 m from the source.

The records of the profile were processed in order to individuate the reflection from the top of the tuff and other deeper events in the pyroclastic series, possibly in the depth range of the cavity. The traces were deconvolved to increase their temporal resolution. To get rid of unwanted coherent noise (such as ground roll and air wave) and random noise, F-K dip filtering and digital band-bass filtering were also done; then NMO correction was applied (all the filter parameters and the NMO velocity functions are described in the captions). Note that on record n. 5 in Fig. 10, the last four traces are dead, because the geophones were not connected in the field for lack of space. These dead traces were maintained during processing in order to have a control on any noise generated by the processing sequence itself. We noticed in fact that some algorithms, in particular F-K filtering, can create unwanted artificial events; this is also reported by a large number of authors working with these filters. In Fig. 12, for example, it can be seen that some low-level noise has been propagated into the dead traces. We tried many parameters and different fan widths in input to the F-K filter, but were not able to entirely suppress this noise. This shows that F-K dip filtering should be used carefully.

The profile with only 200-Hz high-cut filtering and NMO correction is displayed in Fig. 11, where the reflection from the top of the tuff is evidenced on the plot. No other reflected events

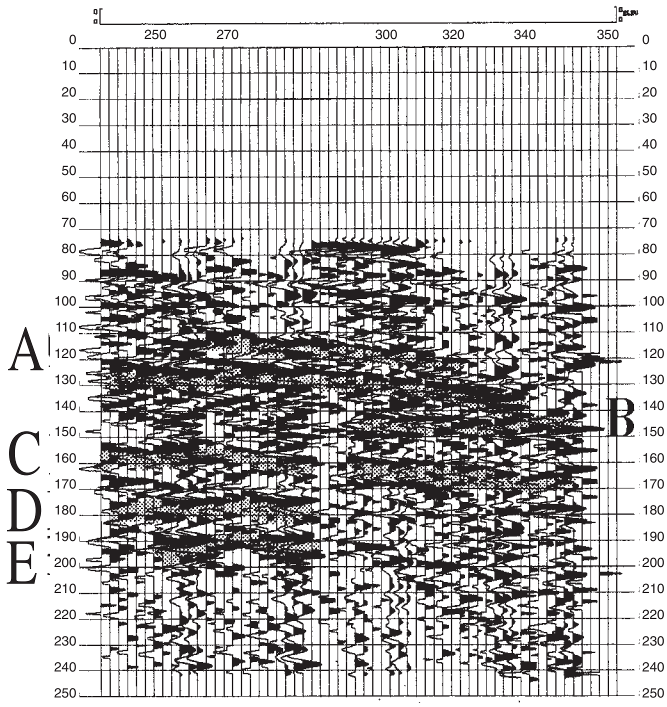

Fig. 12 - Final single-fold section for the site of Frattaminore with deconvolution (prewhitening: 10%; filter lenght: 64 ms; window: 90-250 ms) , F-K filtering (1.2-3 ms/trace), 200 Hz digital filtering and NMO correction (800 m/s) applied. Most of the events, labelled from A to E, are discontinuous and show a light dip toward the right of the profile. Note that the reflection from the top of the tuff, well visible in Fig 9, had to be destroyed in order to eliminate also the ringing associated to it that hides the deeper events. The strongest of all the events (labelled A), which is visible at around 110-120 ms on the left side of the profile, has been associated with the velocity change into the yellow tuff. The event identified as (C), at 160 ms, could be the reflection from the bottom of the tuff that in the area is around 30-40 m thick. For both these events there is a clear enough evidence of their existence even on the unprocessed data of figure 9. For all the other events identified as (B), (D) and (E), this evidence is very little or insufficient and perhaps they could be created the processing sequence applied to the data. Furthermore, on this plot there is no convincing evidence of the presence of energy diffracted from the cavity.

are clearly visible on it, due the ringing of the signal and the presence of coherent noise. A plot of the same profile after processing is presented in Fig. 10. Note that most of the ringing and ground roll energy have been eliminated from the seismogram. Moreover, because the deconvolution, and especially the F-K filtering, were targeted to enhancement of deeper events, they have almost completely destroyed the 80-ms reflection. This was necessary to suppress the ringing on the traces, most of which was generated (and had the same dip) by the 80-ms reflection. Finally, in this plot, some other events deeper than the reflection from the top of the tuff can be identified and evidenced. Most of them show a slight dip (around 6-8 degrees) toward the right of the section. The first is visible between 110 and 120 ms, on the left side of the plot, and is labelled with the letter (A). Another event (B) arrives only in the right half of the plot, at around 140-150 ms. A more continuous deeper reflection (C) has a two-way time of circa 160 ms and seems to possess a more complex morphology. Finally other two discontinuous events at 170 (D) and 190 ms (E) were evidenced.

The event (C) could be the reflection from the bottom of the tuff formation, which in the area is around 30-40 m thick. The other reflections could be caused by the velocity change entering (A) and exiting the Yellow Tuff Formation. There is no clear evidence of reflections from the depth range (80-90 ms) of the cavity.

We cannot be completely sure that all these events are real and not created by the processing sequence. On the original section there are slight traces of the 120-ms reflection, and perhaps some traces of the 160-ms reflection. All the other events individuated in Fig. 12 cannot be seen on the unprocessed section of Fig. 11 because of the ringing. On the other hand, we could not drill well at the site, as this was on private property. However, considering that the data are single fold, and that they were collected with an 8-bit seismograph, the results obtained were beyond our expectations.

5. Conclusions

Two tests (at Frattaminore and Grumo Nevano) of the potential of the seismic reflection method for the detection of cavities in the Neapolitan Yellow Tuff formation were presented in this paper. Both sites are characterised by very similar geological conditions, and have a cavity buried a few meters below the top of the tuff formation which, in both sites, is covered by a sequence of loose pyroclastic terrain. At Frattaminore we could see on the seismic records some diffraction hyperbolae generated by the seismic response of the cavity. Assuming that the diffraction hyperbola was generated at the roof of the cavity, and assuming an average velocity of 400 m/s for it, the depth calculated (16.5 m) is very close to its actual position (13±2 m). Unfortunately, software (other than standard migration) to enhance diffractions at the expense of everything else has not yet been fully developed. At the same site, we were able to spot the reflection from the top of the tuff on the field data. Additional processing of the data was needed to enhance other deeper reflections inside the volcanic series. At Grumo Nevano, on the other hand, we were not able to record seismic data of good quality, despite the following circumstances:

1. a considerable geological similarity to the Frattaminore site;
2. a denser spatial and temporal data sampling;
3. even more favourable theoretical conditions for the location of the cavity (the cavity of Grumo is located farther from the tuff/overburden interface).

We think that these contrasting results obtained from geologically similar places, where the data were collected using the same instrumentation, source, and techniques, are extremely instructive for understanding the potentials and the limitations of the seismic reflection method for the detection of cavities buried in pyroclastic rocks. There are some geographical areas where good data cannot be obtained; that is, reflection seismology just does not work there. This problem is common to many other geophysical methods. Even in areas where good data are expected, it is always possible to obtain bad or no data. Every area has its own character; thus, what works in some circumstances will not necessarily work elsewhere. Therefore it is desirable to design data acquisition parameters for obtaining the best quality data possible for a given objective. It is particularly important not to assume that computer processing will cure all data ailments. Seismic data acquisition equipment has finite capabilities (Knapp and Steeples, 1986). Computer processing can enhance tremendously the data, but all depends on the original quality of the data. The computer cannot make bad data appear good (Knapp and Steeples, 1986).

In conclusion, the problem of cavity location has no simple solution. The best way to tackle it, is to compare the results of many different geophysical methods. Geoelectric, georadar and microgravimetry profiles, as well as reflection seismic surveying and a fan of refraction surveys in a area can give much varied information when looking for an underground cavity. Abundance of geophysical data helps to create a database of great spatial and temporal density, and produce more decisive elements.

Acknowledgement. This work was done as part of a more general program of acquisition, processing and interpretation of shallow seismic reflection data, on which the authors are working. We thank the CNR and the Ministry for University and Scientific Research for their financial support (contracts CNR 94 01618, MURST 40% 92 and MURST 60% 93 to A. Rapolla). We also thank our referees for their very favourable comments on the paper and their precious advice.

References

Clayton R. W. and Engquist B.; 1977: *Absorbing boundary conditions for acoustic and elastic wave equations.* Bull. Seism. Soc. Am., **67**, 1529-1540.

Keys R. G.; 1985: *Adsorbing boundary conditions for acoustic media.* Geophysics, **50**, 892-902.

Kelly K. R., Alford R. M. and Whitmore N. D.; 1982: *Modeling - The forward method.* In: Jain K. and deFigueiredo R. (eds), Concepts and Techniques in Oil and Gas Exploration. Soc. Expl. Geophys.

Keiswetter D., Black R. and Schmeissner C.; 1995: *A program for seismic wavefield modeling using finite-difference techniques.* Computers and Geosciences, **22**, 267-286.

Knapp R. W. and Steeples D. W.; 1986: *High resolution comon depth point seismic reflection profiling: Instrumentation.* Geophysics, **51**, 276-282.

Reynolds A. C.; 1978: *Boundary conditions for the numerical solution of wave propagation problems.* Geophysics, **43**, 1099-1110.

Sochacky J., Kubichek R., George J., Fletcher W. R. and Smithson S.; 1987: *Adsorbing boundary conditions and surface waves.* Geophysics, **52***,* 60-71.

Yilmaz O.; 1987: *Seimsic Data Processing.* Investigations in Geophysics, n. 2., Soc. Expl. Geophys. 526 pp.